Polarization analysis equipment in SANS-J-II: Study of polymer electrolyte membrane for fuel cell

by Ananda Putra

PNCMI 2012 – Polarized Neutrons for Condensed Matter Investigations 2012

Polarization analysis equipment in SANS-J-II: Study of polymer electrolyte membrane for fuel cell

Yohei Noda[a], Daisuke Yamaguchi[a], Ananda Putra[a], Satoshi Koizumi[b], Yoshifumi Sakaguchi[c], Takayuki Oku[d], and Jun-ichi Suzuki[c,d]

[a]Quantum Beam Science Directorate, Japan Atomic Energy Agency, Ibaraki 319-1195, Japan
[b]College of Engineering, Ibaraki University, Ibaraki 316-8511, Japan
[c]Comprehensive Research Organization for Science and Society, Ibaraki 319-1106, Japan
[d]J-PARC Center, Japan Atomic Energy Agency, Ibaraki 319-1195, Japan

Abstract

In small angle neutron scattering spectrometer, SANS-J-II at Japan Research Reactor No. 3 (JRR-3), a polarization analysis setup has been equipped, which is composed of transmission-type supermirror polarizer, radial-bender-type supermirror analyzer, π flipper, and solenoids for generating guide magnetic field. This setup was applied to the structural study of polymer electrolyte membrane, Nafion under water-swollen state. The sample is known to exhibit several characteristic peaks at wide angle region, which is related to water transporting channels. By use of polarization analysis technique, the coherent and incoherent contributions were successfully separated. Consequently, we obtained reliable information about decaying power law of ionic cluster peak and the shape of the broad peak, relating to ordering with short distance (5.6 Å).

1. Introduction

Polarization analysis is useful for the precise reduction of incoherent scattering due to protons in a sample [1,2]. This technique has been effectively applied to the study of atomic-level structure of polymers [3,4], since incoherent scattering contributes significantly at wide scattering angle.

For polarization analysis, ^{3}He spin filter has been increasingly used in these days, because of its recent remarkable improvement [5-9]. On the other hand, for the same purpose, solid state analyzer composed of supermirror has also been used effectively, for a longer time [10-12]. Though its initial cost, mainly for large number of supermirror sheets, is rather expensive, its maintenance cost is extremely low.

Small angle neutron scattering (SANS) spectrometer, SANS-J-II [13-15] in Japan Research Reactor No. 3 (JRR-3) has been equipped with radial-bender-type supermirror analyzer [10-12]. Combining it with a transmission-type supermirror polarizer, solenoid coils for generating guide magnetic field, and π flipper, we can realize polarization analysis.

We applied this setup for the structural study of Nafion film swollen by water. Nafion has been widely used as electrolyte membrane for various applications, such as fuel cell, because of its high proton conductivity, high chemical stability, and high mechanical strength. It is composed of hydrophobic main chain ($-CF_2-$) and hydrophilic side-chain end ($-SO_3H$) (Fig. 1a). As a result, phase-separated structure (which is called ionic cluster) is formed to work as a pathway of water or ions. For investigating this structure, SANS has been used intensively, but its morphology is still under debate [16-20]. Recently, Molecular Dynamics (MD) simulation indicated characteristic ordering in short distance (5.6Å), in addition to ordering due to ionic cluster (40Å) [21]. It was suggested that the study of atomic-level structure will give a new insight to the ionic cluster formation. However, the analysis of the corresponding wide angle scattering has been bothered by the difficulty in the precise determination of the incoherent scattering, because of the easily fluctuating water content in thin film sample, which is necessary for calculating the amount of incoherent scattering. For this type of study, *in situ* determination of the incoherent scattering by use of polarization analysis technique is thought to be an ideal solution.

2. Experimental

As a sample, Nafion 112 film with 0.05 mm thickness purchased from *DuPont*, was used. The sheet with 30mm × 30mm area was rolled and fixed inside an aluminum cylinder (inner diameter is 5mm) with a sealing cap, on the sample stage. The bottom part of the cylinder was filled with water, to which the lower part of the sample film contact, so that the water content in the sample became constant through the experiment.

Fig. 1b indicates polarization analysis setup in SANS-J-II [13-15]. Neutron beam with a wavelength of 6.5 ± 0.6 Å was polarized up to 98.5%, by use of transmission-type Fe/Si supermirror polarizer of $m = 2.5$ (m indicates a factor of the critical angle for neutron reflection in relation to Nickel). The polarized neutron beam flied along the central axis of solenoids, which generated guide magnetic field to avoid the neutron spin depolarization. In some cases, the neutron polarization was inverted by use of Drabkin-type, two-coil π flipper (not shown in the figure). When the π flipper inverted the neutron polarization, its magnitude slightly decreased (~96.7 %). The subsequent polarized neutron with 8mm diameter was illuminated into the sample.

The scattered neutron from the sample was accepted by a supermirror-radial-bender-type analyzer [10-12], fixed in front of the position-sensitive detector. The analyzer was designed by P. Böni and fabricated by *Swiss Neutronics*. We purchased this from *Avance* (Japanese agent of *Swiss Neutronics*). It's composed of 70 sheets of supermirror, coated with FeCoV/TiN$_x$ in both sides ($m = 2.5$ for the concave side, $m = 1.5$ for the convex side). As shown in upper part of Fig. 1b, supermirror-coated borofloat glass substrates were slightly bended so that the scattered neutron from the inlet can pass through only after the spin-
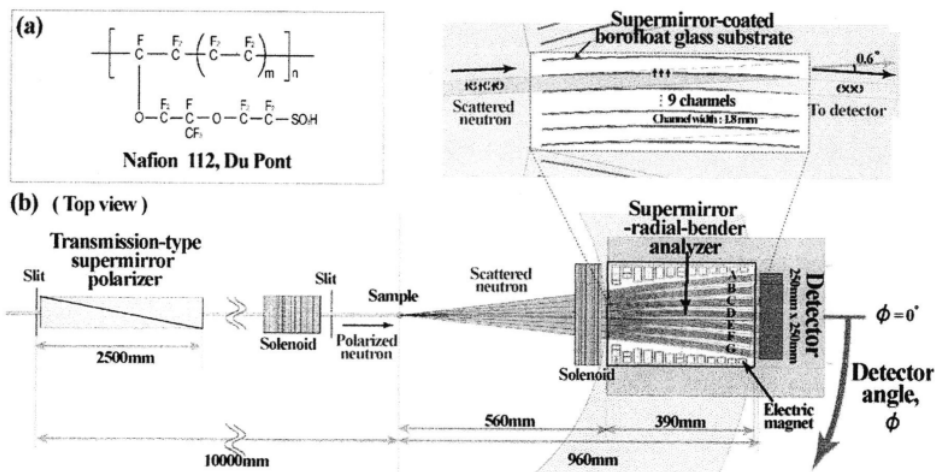
Fig. 1. (a) Chemical structure formula of Nafion 112. (b) (Lower part) Schematic top view picture of the polarization analysis setup in SANS-J-II. (Upper part) Zoomed picture of a supermirror polarizing bender, indicating a spin-selective filtering process.

selective reflection on the supermirror-coated surface. Non-reflected neutrons were captured by boron nuclei in borofloat glass. Finally, the spin-selected neutrons from the outlet of the analyzer were detected by the position-sensitive detector. The position-sensitive detector and the analyzer was fixed on the same stage, which can move around a sample with keeping the distance from the sample to be constant. For other experimental setups, this analyzer can slide out of the beam line.

For this instrument, when the π flipper was not energized, the neutron polarized by the upstream polarizer was filtered out by the analyzer. For this case, we can detect only neutrons with its spin inverted by scattering [spin-flipping (SF) setup]. On the other hand, when the π flipper was energized, we can detect only neutrons with its spin not inverted by scattering [non-spin-flipping (NSF) setup].

The angular distribution of the scattered neutrons was measured by the position-sensitive detector with changing the detector angle, Φ, from 0° (beam center) to 30° at the interval of 2°. The reason for this detector angle scanning, with small angle steps, will be mentioned later. The measurement was conducted for both of NSF and SF setups.

3. Results and discussion

3.1. Data reduction

Fig. 2a shows the obtained 2-dimensional distribution of the scattered neutrons. The color brightness indicates the frequency of neutron counting rate. The clear difference between NSF and SF setups was observed. The obtained images indicate bright vertical strips, indicated by white frames, corresponding to the neutrons coming out from the outlet of the analyzer bender, labeled A to G. The gap between the bright vertical strips will cause a discontinuity in the observed scattering angle, especially at wide angle region. For recovering this situation, the measurements were conducted with small angle steps, as mentioned in the experimental part.
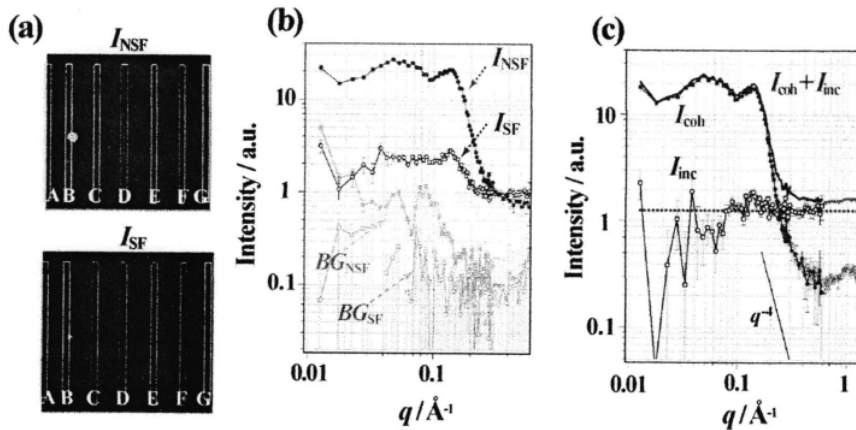
Fig. 2. (a) 2-dimensional distribution of the neutrons scattered from the water-swollen Nafion sample on the detector plane with the size of 250mm × 250mm, with $\Phi = 4°$. The color brightness corresponds to the frequency of neutron counting rate. The upper and lower images were obtained for the NSF and SF setups, respectively. The letters A to G indicate the position of the outlet of the corresponding benders, A to G. The white rectangular frames indicate the effective area, used for the analysis. (b) Totally averaged one-dimensional scattering profiles as a function of q. I_{NSF} (red filled circle) and I_{SF} (blue open circle) indicate the sample's profile measured at the NSF and SF setups, respectively. BG_{NSF} (light red filled rectangle) and BG_{SF} (light blue open rectangle) are for the empty cell. (c) Separated coherent (I_{coh}, red filled circles) and incoherent (I_{inc}, blue open circles) scattering contributions, and the sum of the two ($I_{coh} + I_{inc}$, purple line). The gray curve added in the high q side ($q > 0.5$ Å^{-1}) indicates the profile obtained by use of unpolarized neutron beam. By subtracting the determined incoherent scattering (dashed gray line) from this, the coherent contribution (gray circles) was determined.

For these two-dimensional images, circular averaging calculation should be applied in order to obtain one-dimensional profiles as a function of a magnitude of scattering vector, q [$= (4\pi/\lambda)\sin(\theta/2)$, here, λ is neutron wavelength, and θ is scattering angle.]. In this calculation, we only counted the scattered neutrons inside the strips. The employed scheme is like point-to-point scanning using 7 point detectors especially at high scattering angle region, although at lower angle the scattered neutron distribution is position-sensitive inside the strips. In this calculation, we neglected the strips A and G, because they are near the detector frame, where counting efficiency was inhomogeneous. Consequently, 5 circular averaged profiles were obtained (not shown in the figures), and coincided well with each other. Finally, the totally averaged profiles (I_{NSF} and I_{SF}, for the NSF and SF setups, respectively) was obtained with good counting statistics (Fig. 2b).

The obtained I_{NSF}, to which coherent scattering mainly contributes, exhibited two clear peaks. This is in good accordance with previously reported results, where the peaks at $q = 0.05$ Å^{-1} and $q = 0.14$ Å^{-1} were attributed to the interference among crystalline domains and that among ionic clusters, respectively [17].

Fig. 2b also shows the background scattering profiles (BG_{NSF} and BG_{SF}) of the empty cell. For both of NSF and SF setups, the background was less than 1/10 of the sample scattering.

3.2. Separation of coherent and incoherent scattering

According to the literature [2], I_{NSF} and I_{SF} are given by the following equations.

$$I_{NSF} = I_{coh} + (1/3)\, I_{inc}, \qquad (1)$$

$$I_{SF} = (2/3)\, I_{inc}. \qquad (2)$$

Here, I_{coh} and I_{inc} indicate the coherent and incoherent scattering, respectively. These equations mean that coherent scattering does not change neutron spin direction, but incoherent scattering inverts neutron spin direction with a probability of 2/3. With considering the experimental imperfection, the following equations are given.

$$I_{NSF} = [(1 + P_{all}) / 2]\, [I_{coh} + (1/3)\, I_{inc}] + [(1 - P_{all}) / 2]\, [(2/3)\, I_{inc}], \qquad (3)$$

$$I_{SF} = [(1 + P_{all}) / 2]\, [(2/3)\, I_{inc}] + [(1 - P_{all}) / 2]\, [I_{coh} + (1/3)\, I_{inc}]. \qquad (4)$$

Here, P_{all} is the overall analyzing power of the polarizer-analyzer combination, and given by the following equation.

$$P_{all} = (N_{NSF}{}^{0} - N_{SF}{}^{0}) / (N_{NSF}{}^{0} + N_{SF}{}^{0}). \qquad (5)$$

Here, $N_{NSF}{}^{0}$ and $N_{SF}{}^{0}$ indicate the direct beam intensity observed for the NSF and SF setups, respectively. Solving the equations (3) and (4) for I_{coh} and I_{inc}, we obtain the following equations.

$$I_{coh} = [(P_{all} + 3) / (4P_{all})]\, I_{NSF} + [(P_{all} - 3) / (4P_{all})]\, I_{SF}, \qquad (6)$$

$$I_{inc} = [3(P_{all} - 1) / (4P_{all})]\, I_{NSF} + [3(P_{all} + 1) / (4P_{all})]\, I_{SF}. \qquad (7)$$

By applying the experimentally determined P_{all} of 0.86 to the equations (6) and (7), I_{coh} and I_{inc} were separated as shown in Fig. 2c. Though the obtained I_{inc} fluctuated at the low q side ($q < 0.05$ Å^{-1}), it was flat elsewhere. This indicated that the polarization analysis properly worked, since I_{inc} should be q-independent. In the obtained I_{coh}, we can clearly see the decaying power law of the ionic cluster peak at $q = 0.14$ Å^{-1}.

In Fig. 2c, the gray curve in the high q side ($q > 0.25$ Å^{-1}) indicates the profile measured with unpolarized neutron beam, without the analyzer. It agreed well with the calculated $I_{inc} + I_{coh}$, in the overlapping region. By subtracting the determined incoherent scattering (shown by the dotted gray line in Fig. 2c), we calculated the coherent scattering (gray open circles) for this extended high-q region. As a result, we can clearly see the shape of the peak at $q = 1.1$ Å^{-1}, due to the atomic-level ordering.

In this time, polarization analysis measurements were conducted in the limited q region up to $q = 0.6$ Å^{-1}, because of the limited beam-time. So, the determined I_{inc} was extrapolated to larger q. However, due to the higher I_{inc} than I_{coh} there, the subtracted I_{coh} still contains much error. The extension of polarization analysis measurement to this high q region is required for improving the signal-to-noise ratio. This should be our future work.

4. Conclusion

For water-swollen Nafion film, we applied polarization analysis technique for precisely reducing incoherent scattering. The observed 2-dimensional neutron scattering distribution indicated 7 strips corresponding to the scattered neutrons passing through 7 bender packages. This specific situation was recovered by detector angle scanning with small angle steps. Finally, the coherent and incoherent

contributions were separated successfully. The separated q-independent I_{inc} indicated that the experiment was properly conducted. In the separated coherent scattering, the decaying power law of ionic cluster peak was evaluated precisely. Furthermore, subtracting the determined I_{inc} from the profile obtained with unpolarized neutron beam, the shape of the peak at $q = 1.1$ Å^{-1} became clear. In conclusion, we think *in situ* determination of incoherent scattering by polarization analysis technique is very advantageous for the study of water-swollen film samples, whose water content is difficult to be evaluated.

Acknowledgements

References

[1] Moon RM, Riste T, and Kohler WC, *Phys. Rev.* 1969;**181**:920-931.

[2] Dore JC, Clarke JH, and Wenzel JT, *Nucl. Instrum. Methods Phys. Res. Sect. A* 1976;**138**:317-319.

[3] Lamers C, Schärpf O, Schweika W, Batoulis J, Sommer K, and Richter D, *Physica B* 1992;**180-181**:515-518.

[4] Gelix AC, Arbe A, Alvarez F, Colmenero J, Schweika W, and Richter D, *Macromolecules* 2006;**39**:3947-3958.

[5] Gentile TR, Jones GL, Thompson AK, Barker J, Glinka CJ, Hammouda B, and Lynn W, *J. Appl. Cryst.* 2000;**33**:771-774.

[6] Ino T, Nakamura M, Oku T, Shinohara T, Suzuki J, Ohoyama K, and Hiraka H, *Physica B* 2009;**404**:2667-2669.

[7] Kira H, Sakaguchi Y, Oku T, Suzuki J, Nakamura M, Arai M, Kakurai K, Endoh Y, Arimoto Y, Ino T, Shimizu HM, Kamiyama T, Tsutsumi K, Ohoyama K, Hiraka H, Yamada K, and Chang LJ, *Physica B* 2011;**406**:2433-2435.

[8] Sakaguchi Y, Kira H, Oku T, Shinohara T, Suzuki J, Sakai K, Nakamura M, Aizawa K, Arai M, Noda Y, Koizumi S, Takeda M,Endoh Y, Chang LJ, Arimoto Y, Ino T, Shimizu HM, Kamiyama T, Ohoyama K, Hiraka H, Tsutsumi K, Yamada K, and Kakurai K, *J. Phys.: Conf. Ser.* 2011;**294**:012017/1-012017/7.

[9] Ioffe A, Babcock E, Mattauch S, Pipich V, Radulescu A, and Appavou MS, *Chin. J. Phys.* 2012;**50**:137-154.

[10] Schärpf O, *Physica B* 1989;**156-157**:639-646.

[11] Böni P, Clemens D, Senthil Kumar M, and Pappas C, *Physica B* 1999;**267-268**:320-327.

[12] Semadeni F, Roessil B, and Böni P, *Physica B* 2001;**297**:152-154.

[13] Koizumi S, Iwase H, Suzuki J, Oku T, Motokawa R, Sasao H, Tanaka H, Yamaguchi D, Shimizu HM, and Hashimoto T, *J. Appl. Cryst.* 2007;**40**:s474-s479.

[14] Oku T, Iwase H, Shinohara T, Yamada S, Hirota K, Koizumi S, Suzuki J, Hashimoto T, and Shimizu HM, *J. Appl. Cryst.* 2007;**40**:s474-s479.

[15] Iwase H, Koizumi S, Suzuki J, Oku T, Sasao H, Tanaka H, Shimizu HM, Hashimoto T, *J. Appl. Cryst.* 2007;**40**:s414-s417.

[16] Lee EM, Thomas RK, Burgess AN, Barnes DJ, Soper AK, and Rennie AR, *Macromolecules* 1992;**25**:3106-3109.

[17] Kim MH, Glinka CJ, Grot SA, and Grot WG, *Macromolecules* 2006;**39**:4775-4787.

[18] Iwase H, Koizumi S, Iikura H, Matsubayashi M, Yamaguchi D, Maekawa Y, and Hashimoto T, *Nucl. Instrum. Methods Phys. Res. Sect. A* 2009;**605**:95-98.

[19] Putra A, Iwase H, Yamaguchi D, Koizumi S, Maekawa Y, Matsubayashi M, and Hashimoto T, *J. Phys.: Conf. Ser.* 2010;**247**:012044/1-012044/11.

[20] Hasegawa S, Takahashi S, Iwase H, Koizumi S, Morishita N, Sato K, Narita T, Ohnuma M, and Maekawa Y, *Polymer* 2011;**52**:98-106.

[21] Brandell D, Karo J, and Thomas JO, *Journal of Power Sources* 2010;**195**:5962-5965.

Polarization analysis equipment in SANS-J-II: Study of polymer electrolyte membrane for fuel cell